Nuclear Physics A533 (1991) 749–760
North-Holland

NUCLEAR
PHYSICS A

PION PRODUCTION WITH RADIOACTIVE NUCLEI

Bao-An LI, Mahir S. HUSSEIN[1] and Wolfgang BAUER

National Superconducting Cyclotron Laboratory, East Lansing, MI 48824-1321, USA
and
Department of Physics and Astronomy, Michigan State University, East Lansing, MI 48824-1321, USA

Received 18 March 1991
(Revised 30 May 1991)

Abstract: The possibility to study the coordinate and momentum space structure of exotic nuclei via pion production with radioactive beams is investigated. Exploratory calculations for ^{11}Li are presented. A strong sensitivity of the pion energy spectra to the momentum distribution of the halo neutrons is found.

1. Introduction

Exotic radioactive isotopes close to the neutron drip line provide us with a unique opportunity to study the transition region between nuclear matter and neutron matter and its equation of state. This is the main nuclear physics reason for the production of radioactive beams and their use for nuclear reaction studies [1–3]).

A pioneering effort in using radioactive beams was carried out by Tanihata and collaborators at the Bevalac. They studied the total reaction cross sections of several Li and Be isotopes with beams of energies around 800 MeV/nucleon produced in projectile fragmentation reactions [4,5]). For the isotopes ^{11}Li and ^{14}Be, they found anomalously large reaction cross sections and nuclear radii associated with these cross section, which were much larger than expected from a simple $A^{1/3}$ parameterization.

This effect can be understood from the argument that the very last member of each isotope sequence as we reach the limit of stability will be weakly bound. Due to the small binding energy and the Heisenberg uncertainty principle, the tail of the wave function is expected to extend far out beyond the normal nuclear matter radius expected from an $A^{1/3}$ Parameterization.

Present state-of-the-art self-consistent Hartree–Fock or shell model nuclear-structure calculations are not able to correctly reproduce the binding energy of ^{11}Li or ^{14}Be. However, it is possible to numerically adjust the binding energy to the measured experimental values. In this case, one is able to reproduce the large observed interaction

[1] Permanent address: Instituto de Física, USP, C.P. 20516, 01498, São Paulo, S.P., Brazil.

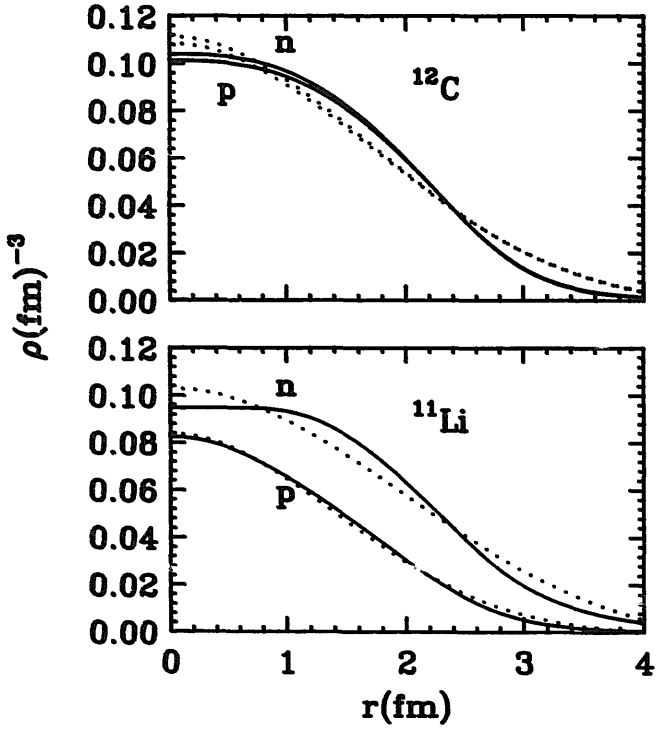

Fig. 1. Density distributions for ^{12}C and ^{11}Li. The solid lines are calculated with the binding energy adjusted shell model. The dotted lines are the gaussian fits to the density profiles.

radii with reasonable accuracy [6]). The proton and neutron matter densities obtained in this way are represented by the solid lines in the lower part of fig. 1.

Due to the small binding energy and the large spatial extension of the neutrons in the so-called "halo" [7]), one expects the neutron momentum distribution to exhibit a smaller width than in more deeply bound nuclei. This has indeed been observed in several ways.

Kobayashi *et al.* [8]) observed the fragmentation of ^{11}Li with a radioactive beam of energy 790 MeV/nucleon. Their experimental data for the transverse momentum distribution of ^{9}Li from the reaction $^{11}\mathrm{Li} \rightarrow {}^{9}\mathrm{Li} + 2\mathrm{n}$ can be found in the bottom half of fig. 2. It can be fitted with a superposition of two gaussian distributions of widths $\omega_{\mathrm{core}} = 95 \pm 12$ MeV/c and $\omega_{\mathrm{halo}} = 23 \pm 5$ MeV/c. By using Goldhaber's statistical model of the fragmentation process [9]), they were able to interpret the two widths as an indication that the neutron momentum distribution inside the halo and the core of ^{11}Li are different. However, alternative explanations of the two-widths shape of the transverse momentum distribution are possible [10]). It is therefore necessary to pursue other complementary ways of determining the momentum and coordinate space structure of exotic nuclei.

For example, one can also measure the neutron momentum distribution in ^{11}Li by detecting the neutrons from the decay of ^{11}Li. This is presently being pursued by Anne *et al.* [11,12]).

In this paper, we will investigate the possibility to further determine the coordinate and momentum space distribution of neutrons inside weakly bound isotope via pion production with radioactive beams.

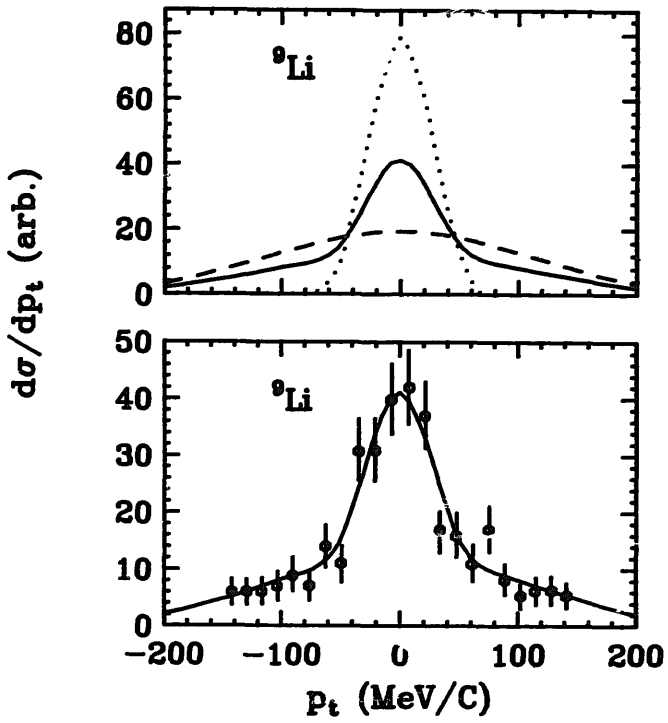

Fig. 2. Upper figure: Calculated transverse momentum distribution of ^{9}Li in the reaction ^{11}Li + ^{12}C → ^{9}Li + 2n + X. The dashed (dotted) line is obtained by assuming knock-out of two neutrons from the core (halo) of ^{11}Li. The solid line represents the weighted sum of the two. Lower figure: Comparison with the experimental data.

The paper is organized as follows: In the next section, we discuss the inclusive π^+ and π^- production cross sections in reactions of radioactive beams in the context of a Glauber-type multiple collision model. We focus on the possibility of probing the difference between proton and neutron densities by studying the ratio of π^+ and π^- production cross sections. Sect. 3 contains our results regarding the pion energy spectra studied within a modified Fermi-gas model. We conclude with a summary in the last section.

2. Inclusive π^+ and π^- production cross section

In principle, pion production in nucleus–nucleus collisions can be described with nuclear transport models developed during the last decade [13–15]). These models have been very successful to describe particle production in heavy-ion collisions. However, they are semi-classical in nature and therefore lack the capability to properly take into account the special nuclear structure features of weakly bound nuclei near the drip line. It is therefore necessary to construct a more phenomenological model. The model we present in the following is not able to provide a complete time-dependent description of heavy-ion reactions the way the above mentioned transport models can. But our model is more precise as far as utilizing nuclear structure information is concerned. In the following, we perform a calculation similar to the one presented by Lombard

and Maillet [21,22]), but using shell-model nucleon densities and energy-dependent cross sections.

2.1. THE MODEL

Within a Glauber-type multiple collision model, the total number of nucleon–nucleon collisions in the reaction of A + B at an impact parameter b is

$$N(b) = \bar{\sigma}(E) \int_{\mathrm{O}} \mathrm{d}x\,\mathrm{d}y \int \mathrm{d}z_1\,\mathrm{d}z_2\,\rho_{\mathrm{A}}(x,y,z_1)\rho_{\mathrm{B}}(x,y-b,z_2)\,, \tag{1}$$

where O is the overlap region of nuclei A and B, and $\bar{\sigma}(E)$ is the momentum-averaged total nucleon–nucleon cross section. Since the core nucleons and the halo neutrons have different momentum distributions in ^{11}Li, $\bar{\sigma}(E)$ may be written as

$$\bar{\sigma}(E) = \tfrac{9}{11}\bar{\sigma}_{\mathrm{core}}(E) + \tfrac{2}{11}\bar{\sigma}_{\mathrm{halo}}(E)\,. \tag{2}$$

Since we wish to analytically carry out the bulk of our calculations, we follow Karol [16]) and assume that the nucleon density distribution is a gaussian function

$$\rho(r) = \rho(0)\exp\left(-\frac{r^2}{a^2}\right). \tag{3}$$

The integration in eq. (1) can then be performed analytically to yield the result

$$N(b) = \frac{\bar{\sigma}(E)\pi^2\rho_{\mathrm{A}}(0)\rho_{\mathrm{B}}(0)a_{\mathrm{A}}^3a_{\mathrm{B}}^3}{a_{\mathrm{A}}^2+a_{\mathrm{B}}^2}\exp\left(-\frac{b^2}{a_{\mathrm{A}}^2+\alpha_{\mathrm{B}}^2}\right). \tag{4}$$

Similar forms for the proton–proton and neutron–neutron collision numbers can be obtained in terms of their density distribution parameters.

Under the assumption that pions are produced through Δ-resonances, the inclusive π^+ and π^- cross sections can then be written as [22])

$$\begin{aligned}
\frac{\mathrm{d}\sigma_{\mathrm{inc}}^{\pi^+}}{\mathrm{d}\Omega} &= |f_{N\Delta}(q)|^2 Z_{\mathrm{A}}Z_{\mathrm{B}}\frac{\pi^2\rho_{Z\mathrm{A}}(0)\rho_{Z\mathrm{B}}(0)a_{Z\mathrm{A}}^3a_{Z\mathrm{B}}^3}{a_{Z\mathrm{A}}^2+a_{Z\mathrm{B}}^2}\\
&\quad\times 2\pi\int_0^\infty b\mathrm{d}b\exp\left[-\frac{b^2}{a_{Z\mathrm{A}}^2+a_{Z\mathrm{B}}^2}-\frac{\bar{\sigma}(E)(AB-1)\rho_{\mathrm{A}}(0)\rho_{\mathrm{B}}(0)a_{\mathrm{A}}^3a_{\mathrm{B}}^3}{a_{\mathrm{A}}^2+a_{\mathrm{B}}^2}\right.\\
&\quad\left.\times\exp\left(-\frac{b^2}{a_{\mathrm{A}}^2+a_{\mathrm{B}}^2}\right)\right],\\
\frac{\mathrm{d}\sigma_{\mathrm{inc}}^{\pi^-}}{\mathrm{d}\Omega} &= |f_{N\Delta}(q)|^2 N_{\mathrm{A}}N_{\mathrm{B}}\frac{\pi^2\rho_{N\mathrm{A}}(0)\rho_{N\mathrm{B}}(0)a_{N\mathrm{A}}^3a_{N\mathrm{B}}^3}{a_{N\mathrm{A}}^2+a_{N\mathrm{B}}^2}\\
&\quad\times 2\pi\int_0^\infty b\mathrm{d}b\exp\left[-\frac{b^2}{a_{N\mathrm{A}}^2+a_{N\mathrm{B}}^2}-\frac{\bar{\sigma}(E)(AB-1)\rho_{\mathrm{A}}(0)\rho_{\mathrm{B}}(0)a_{\mathrm{A}}^3a_{\mathrm{B}}^3}{a_{\mathrm{A}}^2+a_{\mathrm{B}}^2}\right.\\
&\quad\left.\times\exp\left(-\frac{b^2}{a_{\mathrm{A}}^2+a_{\mathrm{B}}^2}\right)\right],
\end{aligned} \tag{5}$$

where ρ_{Ni} and ρ_{Zi} are the neutron and proton coordinate space densities of nucleus i, and $f_{N\Delta}(q)$ is the amplitude for the process $N + N \rightarrow N + \Delta$. The exponentials inside the integrals represent the product of the proton (eq. (5)) or neutron (eq. (6)) densities with the elastic survival probability given by

$$\exp\left[-\frac{\bar{\sigma}(E)(AB-1)\rho_A(0)\rho_B(0)a_A^3 a_B^3}{a_A^2+a_B^2}\exp\left(-\frac{b^2}{a_A^2+a_B^2}\right)\right], \tag{6}$$

as derived in ref. [22]).

At beam energies smaller than 1 GeV/nucleon, available experimental data [17,18]) show that pions are mainly produced through Δ-resonances. Direct processes of the form $N + N \rightarrow N + N + \pi$ account for less than 20% percent and higher resonances have negligible cross sections.

From the experimental data of n + p collisions [17]) and the calculated ratio of the isospin matrix elements [22]), it can be shown that the numbers of π^+ and π^- produced in n + p collisions are smaller than that in p + p and n + n collisions, respectively, by about an order of magnitude. We therefore expect that the above equations are good approximations for the present purpose of our calculation.

The above considerations do not include the effect of the Pauli-exclusion principle on the final-state nucleons after producing the pions. This should result in a reduction of $|f_{N\Delta}(q)|^2$ in the nuclear medium. However, to first approximation, this reduction should be the same for both pion species, and, since we are only interested in the ratio of the production cross sections, the reduction factor will cancel out.

Pion reabsorption accounts for up to 50% of the produced primordial pions in the light systems studied here [14]). In the same spirit as just described for the Pauli exclusion principle, the amplitudes $f_{N\Delta}$ should be understood as effective amplitudes which already include this reduction.

2.2. NUMERICAL CALCULATION

Since we are interested in the ratio of the inclusive π^+ and π^- production, the main ingredients in the model calculation are then the density parameters and the momentum-averaged cross sections.

We start out by obtaining realistic density distributions for protons and neutrons for all isotopes under consideration. This is accomplished by using a binding-energy-adjusted shell-model program [6]). As examples for the calculated density distributions, we display in fig. 1 the neutron and proton densities for ^{12}C (upper part) and ^{11}Li (lower part) by the solid lines.

The results of the gaussian fit to the calculated density distributions are represented by the dotted lines. In table 1, we list the obtained values for $\rho(0)$ and a for proton and neutron density distributions for all Li isotopes used in the subsequent calculations as well as the corresponding values for ^{12}C.

TABLE 1
Parameters of the gaussian fits to the nucleon density distributions in Li-isotopes and ^{12}C as calculated by Bertsch, Brown and Sagawa [6])

	$\rho_n(0)$ (fm^{-3})	a_n (fm)	$\rho_p(0)$ (fm^{-3})	a_p (fm)	$\rho(0)$ (fm^{-3})	a (fm)
^{12}C	0.1148	2.110	0.1120	2.128	0.2268	2.120
^{7}Li	0.1051	1.897	0.1121	1.688	0.2168	1.797
^{8}Li	0.1151	1.984	0.0996	1.755	0.2134	1.885
^{9}Li	0.1215	2.071	0.0989	1.760	0.2178	1.952
^{11}Li	0.1115	2.346	0.0851	1.851	0.1922	2.175

For calculating the momentum-averaged nucleon–nucleon cross sections, we choose our momentum space distribution functions such that our results agree with known experimental data.

One such comparison is performed in fig. 2. In the upper part, we use a Fermi-gas model for the momentum distribution of the neutrons in ^{11}Li. We assume different Fermi momenta for core and halo neutrons. The fitted values are $P_F(\text{core}) = 158$ MeV/c and $P_F(\text{halo}) = 38$ MeV/c which coincide with the one inferred from the experimental data by using the Goldhaber model. By randomly picking 2 neutron momenta from within these Fermi spheres and adding their momenta, one obtains a recoil spectrum for ^{9}Li in the projectile rest frame, employing the assumptions entering the Goldhaber model [9]). By picking two neutrons from the halo, one obtains the dotted curve in fig. 2. The dashed curve is the result of using the same procedure on two core neutrons. The solid curve is the result of an addition of the two contributions with the proper weights as measured in the experiment of Kobayashi *et al.* [8]). For purposes of comparison, all curves in the upper part of fig. 2 were normalized to the same value. In the lower part of this figure, we compare the simulated ^{9}Li transverse momentum spectra to the data of Kobayashi *et al.* [8]). One can see that we are able to reliably fit the experimental observables.

We obtain the momentum distribution averaged nucleon–nucleon cross sections by integrating $\sigma(\sqrt{s})$ weighted with the momentum distributions of target and projectile,

$$\bar{\sigma}(E_{\text{beam}}) = \int f_A(\boldsymbol{p}_A) f_B(\boldsymbol{p}_B - \boldsymbol{p}_{\text{beam}}) \sigma(\sqrt{s}(\boldsymbol{p}_A, \boldsymbol{p}_B)) \, d^3p_A d^3p_B \qquad (7)$$

Here, $f_i(\boldsymbol{p})$ are the momentum distributions of target ($i = A$) and projectile $i = B$.

For the purpose of this calculation, we use the well known parameterizations of Cugnon [19]) for the free space elastic and inelastic nucleon–nucleon cross sections as a function of the available center-of-mass energy, $\sqrt{s}$, in a nucleon–nucleon collision.

$$\sigma_{\rm el}(\sqrt{s}) = \frac{35}{1 + 100(\sqrt{s} - 1.8993)} + 20, \qquad \sqrt{s} > 1.8993, \tag{8}$$

$$\sigma_{\rm inel}(\sqrt{s}) = \frac{20(\sqrt{s} - 2.015)^2}{0.015 + (\sqrt{s} - 2.015)^2}, \qquad \sqrt{s} > 2.015. \tag{9}$$

In this parameterization, $\sqrt{s}$ is measured in GeV and σ in mb.

In fig. 3, we display the results for $\overline{\sigma}_{\rm inel}(E_{\rm beam})$ and $\overline{\sigma}_{\rm total}(E_{\rm beam})$ for three different cases. The solid lines are for free nucleons. In this case, the distribution function f are δ-functions, and we have $\overline{\sigma}(E_{\rm beam}) = \sigma_{\rm NN}$. The threshold energy for pion production is in this case $E^{\rm th}_{\rm beam}$/nucleon = 290 MeV.

The dashed and dotted lines represent the case that the target is a carbon nucleus. $f_{\rm A}(p)$ is then a Fermi-gas distribution function with Fermi momentum of 221 MeV/c determined from the carbon fragmentation experiment [20]). The dashed lines are obtained by using the momentum distribution of ^{11}Li core neutrons for $f_{\rm B}$, and the dotted line represents the case that the halo neutron momentum distribution is used. In these cases, the threshold energies for pion production are 70 and 120 MeV, respectively.

One can see from fig. 3 that the distribution averaged value of the total nucleon–nucleon cross section is hardly affected by the momentum distribution of nucleons in target and projectile. However, the averaged inelastic cross section shows a very large effect close to the threshold.

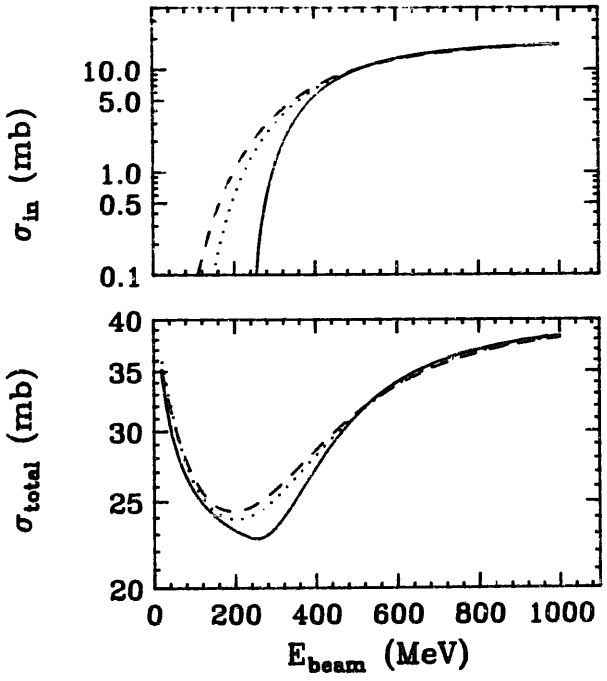

Fig. 3. Nucleon-momentum-averaged nucleon–nucleon cross sections in the reaction ^{11}Li + ^{12}C. Solid lines are the free-space nucleon–nucleon cross sections. Dotted lines are for carbon nucleons colliding with halo neutrons and dashed lines are for carbon nucleons colliding with core nucleons of ^{11}Li.

TABLE 2

Comparison of the computed normalized cross section differences between negative and positive pion production, E, for two different values of $\bar{\sigma}$ and the same quantity obtained from simple counting of nucleons, E_0, for reactions of different Li isotopes with ^{12}C

	$^{7}Li + ^{12}C$	$^{8}Li + ^{12}C$	$^{9}Li + ^{12}C$	$^{11}Li + ^{12}C$
E(40 mb)	0.1153	0.2221	0.2955	0.3951
E(25 mb)	0.1143	0.2210	0.2939	0.3927
E_0	0.1429	0.2500	0.3333	0.4545

In table 2, we present the results of our calculation for the ratio

$$E = \frac{\sigma_{\rm inc}^{\pi^-} - \sigma_{\rm inc}^{\pi^+}}{\sigma_{\rm inc}^{\pi^-} + \sigma_{\rm inc}^{\pi^+}}, \tag{10}$$

for the systems $^{A}Li + ^{12}C$ ($A = 7, 8, 9, 11$) with $\bar{\sigma} = 40$ and 25 mb. These two values for $\bar{\sigma}$ are chosen to represent the case for nucleus-nucleus interactions around the pion production threshold ($E_{\rm beam} \approx 200$ MeV/nucleon $\rightarrow \bar{\sigma} \approx 25$ mb) and for reactions at higher beam energies ($E_{\rm beam} \approx 800$ MeV/nucleon $\rightarrow \bar{\sigma} \approx 40$ mb). For comparison, we also present the ratio E_0 for the two cross section which results from simple counting arguments of neutrons and protons or, equivalently, from assuming that protons and neutrons have the same density distribution in eq. (5),

$$E_0 = \frac{N_A N_B - Z_A Z_B}{N_A N_B + Z_A Z_B}. \tag{11}$$

Our calculations confirm the finding of ref. [21]) that the ratio E is sensitive to the difference between proton and neutron density distribution. However, in our results the effect is small and not quite as dramatic as claimed there. We attribute this to the more realistic density distributions used in our calculations.

3. Pion energy spectra

If we want to study pion energy spectra, it is clearly not sufficient any more to use energy-averaged production cross sections. In the present exploratory study of pion spectra with exotic nuclei, we use a modified Fermi-gas model. It was first used by Bertsch in the study of threshold pion production [23]).

For the individual nuclei, we assume that the phase space distribution function can be separated into coordinate and momentum parts. For the momentum space distribution of the colliding nuclei we use a simplified form of two homogeneously filled Fermi spheres, the centers of which are separated by the beam momentum

$$f_{AB}(\boldsymbol{p}) = \theta(p_{F_A} - |\boldsymbol{p}|)A + \theta(p_{F_B} - |\boldsymbol{p} - \boldsymbol{p}_{\rm beam}|)B. \tag{12}$$

Here p_{F_A} and p_{F_B} are the Fermi momenta of the projectile of mass A and target of mass B, respectively. We will use the Fermi momenta for carbon and ^{11}Li extracted from the experimental data as we have discussed in the previous section.

Pion energy spectra in the reaction A + B can then be calculated as a sum of the pion energy distribution in each nucleon–nucleon collision with all possible momenta within the Fermi spheres

$$\left(\frac{d\sigma_\pi}{dE}\right)_{AB} = C \int \left(\frac{d\sigma_\pi(s)}{dE}\right)_{NN} f_A(p_A) f_B(p_B)\, d^3p_A\, d^3p_B, \tag{13}$$

where C is a constant coming from the integration over the impact parameter, which is irrelevant for the following discussions. s is the square of the center-of-mass energy of the two colliding nucleons.

To calculate the pion energy distribution $(d\sigma_\pi/dE)_{NN}$ in each nucleon–nucleon collision, we assume that pion production is proceeding via the Δ-resonance. The mass distribution of the Δ-resonance is taken from Kitazoe *et al.* [18]) and is given by

$$P(M_\Delta) = \frac{0.25\Gamma^2(q)}{(M_\Delta - M_0)^2 + 0.25\Gamma^2(q)}, \tag{14}$$

where $M_0 = 1232$ MeV, and the width $\Gamma(q)$ of the resonance is parameterized as

$$\Gamma(q) = \frac{0.47q^3}{\left[1 + 0.6(q/m_\pi)^2\right] m_\pi^2}. \tag{15}$$

q is the pion momentum.

The Δ is assumed to be produced isotropically in the nucleon–nucleon center-of-mass frame, and we also assume that the decay of the resonance has an isotropic angular distribution in the Δ rest frame. The decay of the resonance is then calculated using a Monte Carlo integration technique. This leads to a pion energy spectrum in the Δ rest frame which is finally Lorentz transformed into the laboratory frame.

The integration in eq. (13) for calculating the pion spectra in the reaction A + B is performed with the Monte Carlo integration method. Our calculation therefore generates pairs of colliding nucleons from the projectile and the target, and isospin quantum numbers are assigned to these nucleons according to the N/Z ratios of the projectile and the target. We use available experimental data [17,24]) for pion production cross sections in nucleon–nucleon collisions in all possible isospin channels.

One such calculation is performed for the reaction ^{11}Li + ^{12}C at various beam energies. To show the sensitivity of the pion energy spectra on the nucleon momentum distribution of the radioactive nuclei, we show in fig. 4 the π^- spectra calculated by using the core Fermi momentum and halo Fermi momentum for the ^{11}Li projectile, respectively. The solid histograms are calculated with $p_{F_A} = p_F(\text{halo}) = 38$ MeV/c and the dotted histograms are calculated with $p_{F_A} = p_F(\text{core}) = 158$ MeV/c. These two calculations simulate the situations that nucleons coming from ^{12}C collide with the halo and core nucleons of the ^{11}Li, respectively.

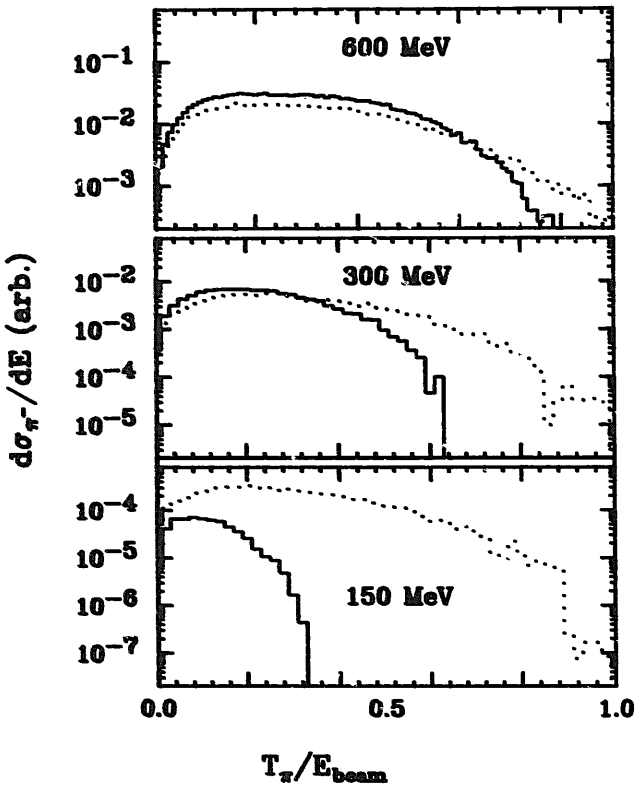

Fig. 4. π^- kinetic energy spectra in the reaction ^{11}Li + ^{12}C at beam energies of 600, 300 and 150 MeV/nucleon. The solid lines are calculated with $p_{F_A} = p_F$(halo) and the dotted lines are calculated with $p_{F_A} = p_F$(core).

A strong sensitivity of the pion spectra to the nucleon momentum distribution can be seen, in particular for beam energies smaller than about 300 MeV/nucleon. Moreover, the different slopes of the two curves indicate that the different momentum distributions of core and halo neutrons can be seen experimentally.

Of course, one needs to know how to disentangle the pions produced by the core and by the halo neutrons. We suggest two ways to proceed: First, one could separate central and peripheral collisions via some impact parameter trigger. Since the halo neutrons should contribute stronger to pion production in peripheral collisions, their effect could probably be isolated. A second and probably more tractable way to isolate the effect of the halo neutrons is a subtraction method. Here one can utilize the fact that a ^{9}Li nucleus contains the same core neutrons as ^{11}Li. Thus, if one subtracts the pion spectrum produced in a ^{9}Li induced reaction from that of a ^{11}Li induced and otherwise identical reaction, the pion spectrum due to the halo neutrons can be obtained.

Presently available radioactive beam facilities can produce high quality ^{11}Li and ^{9}Li beams. Using these, the different neutron momentum distributions of core and halo neutrons in ^{11}Li would then show up as contributions to the pion energy spectra with different slopes in ^{11}Li and ^{9}Li induced reactions. We estimate that a beam of 10^5 ^{11}Li per second at a beam energy of 300 MeV/nucleon would produce about 10^4 pions per

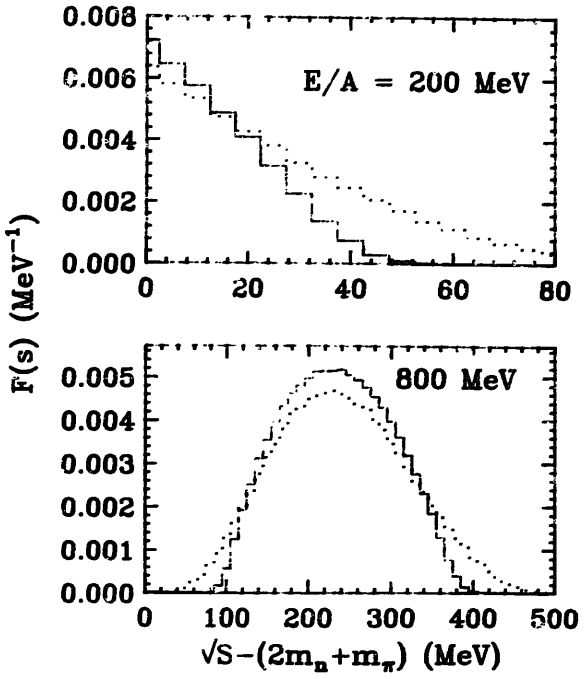

Fig. 5. Distribution of the center-of-mass energy above pion production threshold for pairs of colliding nucleons in the reaction ^{11}Li + ^{12}C. The solid and dotted lines are calculated under the same conditions as in fig. 4.

second. With this production rate, a high quality experiment using a pion spectrometer could be performed.

As can be seen from fig. 4, the difference in the slope of the pion spectra is not so obvious at beam energies above 600 MeV/nucleon. This can be understood by looking at the distribution of the center-of-mass energy, $\sqrt{s}$, of the two colliding nucleons in the reaction A + B

$$F(s) = \int f_A(\boldsymbol{p}_A) f_B(\boldsymbol{p}_B - \boldsymbol{p}_{beam}) \delta(s - 2m_n^2 - 2E_A E_B + 2\boldsymbol{p}_A \cdot \boldsymbol{p}_B)\, d^3p_A d^3p_B. \quad (16)$$

Here we take on-shell nucleons so that $E_i = (p_i^2 + m_n^2)^{1/2}$ for i = A, B.

In fig. 5 we present the distribution of $\sqrt{s} - (2m_n + m_\pi)$, which is the total available center-of-mass energy above pion production threshold in a nucleon–nucleon collisions. The calculation is done for the reaction ^{11}Li + ^{12}C at beam energies of 200 MeV/nucleon and 800 MeV/nucleon. Again, the solid histograms are the results using $p_{F_A} = p_F$(halo) and the dotted ones using $p_{F_A} = p_F$(core). The effect of different internal momentum distributions is obvious at lower energies, but as the beam energy gets much larger than the pion production threshold energy, the effect becomes less obvious.

4. Summary

In summary, we have studied both the coordinate and momentum space structure of the exotic nucleus ^{11}Li with pion production. We use a Glauber-type multiple

collision model calculation for the inclusive π^+ and π^- productions cross sections. By using nucleon densities fitted to shell-model calculations as well as energy-dependent nucleon–nucleon cross sections, it is shown that the ratio of the π^+ and π^- production cross section is sensitive to the difference between the proton and neutron densities.

We calculate in a modified Fermi-gas model for the nucleonic momentum distributions, assume that pion production proceeds mainly via the Δ-resonance, and use the available experimental data for pion productions in nucleon–nucleon collisions. We find that pion energy spectra are strongly sensitive to the internal momentum distribution of halo nuclei like ^{11}Li.

Pion production with radioactive nuclei provides an alternative way for further determination of the properties of exotic nuclei.

We acknowledge G.F. Bertsch, B.A. Brown and A. Sustich for providing us the shell-model densities. This research was supported by the National Science Foundation under Grant Number PHY-8906116, by the CNPq-Brazil, and by BID-USP.

References

1) W. Bauer, Proc. of the Workshop on the science of intense radioactive ion beams, Los Alamos Report LA-11964-C, ed. J.B. McClelland and D.J. Vieira (1990) p. 57
2) I. Tanihata, *in* Treatise on heavy-ion science, vol. 8, ed. D.A. Bromley (1989) p. 443
3) C. Détraz and D.J. Vieira, Ann. Rev. Nucl. Part. Sci. **39** (1989) 407
4) I. Tanihata *et al.*, Phys. Lett. **B160** (1985) 380
5) I. Tanihata *et al.*, Phys. Rev. Lett. **55** (1985) 2676
6) G.F. Bertsch, B.A. Brown and H. Sagawa, Phys. Rev. **C39** (1989) 1154
7) P.G. Hansen and B. Jonson, Europhys. Lett. **4** (1987) 409
8) T. Kobayashi *et al.*, Phys. Rev. Lett. **60** (1988) 2599
9) A.S. Goldhaber, Phys. Lett. **B53** (1974) 306
10) C.A. Bertulani and M.S. Hussein, Phys. Rev. Lett. **64** (1990) 1099
11) R. Anne *et al.*, to be published
12) D. Guillemaud-Müller and A.C. Müller, NSCL Seminars on Experimantal techniques: 1. Exotic nuclei, Michigan State University Report MSUCL-742
13) B.-A. Li and W. Bauer, Phys. Lett. **B254** (1991) 335
14) W. Bauer, Phys. Rev. **C40** (1989) 715
15) W. Cassing *et al.*, Phys. Reports **188** (1990) 363
16) P.I. Karol, Phys. Rev. **C11** (1975) 1203
17) B.J. VerWest and R.A. Arndt, Phys. Rev. **C25** (1980) 1979
18) Y. Kitazoe *et al.* Phys. Lett. **B166** (1986) 35
19) J. Cugnon, T. Mizutani and J. Vandermeulen, Nucl. Phys. **A352** (1981) 505
20) T. Kobayashi, KEK Preprint 89-169
21) R.J. Lombard and J.P. Maillet, Europhys. Lett. **6** (1988) 323
22) A. Tellez, R.J. Lombard and J.P. Maillet, J. of Phys. **G13** (1987) 311
23) G.F. Bertsch, Phys. Rev. **C15** (1977) 713
24) W.O. Lock and D.F. Measday, Intermediate energy nuclear physics (Methuen, London, 1970)